Potential permafrost distribution and ground temperatures based on surface state obtained from microwave satellite data

Christine Kroisleitner[1,2], Annett Bartsch[1,2,3], and Helena Bergstedt[4,2]

[1]Zentralanstalt für Meteorologie und Geodynamik, Vienna, Austria
[2]Austrian Polar Research Institute, Vienna, Austria
[3]b.geos, Korneuburg, Austria
[4]Department of Geoinformatics - Z_GIS, University Salzburg, 5020 Salzburg, Austria

Correspondence to: Annett Bartsch (annett.bartsch@zamg.ac.at)

Abstract.

Land surface state, frozen versus unfrozen conditions, can be captured globally with satellite data obtained by microwave sensors. It has been previously suggested that the number of frozen days per year can be used to determine permafrost extent based on a threshold method. We have tested the validity of the simplification for the northern hemisphere north of 50° and identified regions where more advanced modelling is essential. Coarse spatial resolution microwave satellite data (Metop ASCAT and SSM/I; 12.5km and 25km nominal resolution; 2007 - 2012) which provide the necessary temporal sampling have been used. Borehole measurements across the entire domain as well as a conventional permafrost zone map have been chosen for the assessment of four different methods: 1) quantification of map area overlap, 2) Kendall's τ test with in situ data, 3) in situ data confusion matrix and 4) determination of an empirical relationship between mean annual ground temperature (MAGT) and number of frozen days. The MAGT at coldest sensor depth has been tested for validity to build a comprehensive validation dataset and eventually used for assessment. They have been applied for the determination of an empirical relationship between number of frozen days and MAGT. Uncertainties are low in the continuous permafrost zone except for mountain ranges what might be caused by the coarse spatial resolution. Deviations in transition areas are largest in central Asia and areas with high snow depth. This underlines the importance of snow and suggests that advanced models should be applied in central Asia, including central Yakutia and Mongolia. Mean annual ground temperature can be obtained from ASCAT with an RMSE of 2.2°C compared to 2.5°C in case of SSM/I. This is weaker than what can be obtained using more complex models at medium resolution (appr. 1km), but comparably good taking into account the very coarse spatial resolution of 25km. The average deviation within the validation period is less than one degree Celsius at locations without glaciers and coastlines within the resolution cell. The ASCAT dataset also allows to distinguish between melting and dry snow. The exclusion of snow melt days leads to better results using the selected evaluation method (Pearson correlation) and zonal assessment (by region as well as snow water equivalent classes). Specifically Scandinavia is affected. Further regions which show high differences between the tested methods of potential permafrost extent retrieval are e.g. Western and Central Siberia.

1 Introduction

Permafrost covers large parts of the Earth's surface and is defined as ground that remains at or below 0°C for at least two consecutive years. The impact of climate change on the Arctic, as well as other permafrost dominated environments, is thought to be more severe compared to the rest of the world (Schuur et al., 2015; National research Council, 2013). Warming and with that thawing of permafrost impacts multiple environmental processes ranging from surface and sub-surface hydrology (O'Donnell et al., 2012; Woo et al., 2008), ecological changes (Schuur et al., 2008) to processes like carbon exchange (Hayes et al., 2014). Knowledge of the extent of permafrost and possible changes in it's distribution are therefore crucial for climate modelling and prediction (Cheng and Wu, 2007; O'Connor et al., 2010). So far, the exact extend of permafrost is unknown and has only been approximated (Zhang et al., 2008; Nguyen et al., 2009).

A range of approaches exist for permafrost extent determination. They vary in complexity, accuracy and their parameterization differs depending on the size of the area of interest and data availability. Different temperature data sources are employed for the approximation. E.g. Gruber (2012) uses re-analyses records, which are based on spatially interpolated in situ air temperature data (mean annual air temperature) together with elevation data (laps rate), to generate a global map of permafrost probabilities. Temperature records from re-analyses and land surface temperature from satellites together with basic vegetation information and satellite derived snow properties have been investigated for modelling larger areas by Westermann et al. (2015). Satellite data alone do not provide the required spatially and temporally consistent temperature values. Cloud cover is problematic when using thermal infrared. Clear sky bias is an additional problem (Soliman et al., 2012). Improved temperature records can be obtained for the snow free period from combination with passive microwave data (André et al., 2015) but they need to be complemented with re-analysis data for the remaining year in order to derive the required indices.

A different and simpler approach using only satellite records has been recently described by Park et al. (2016). They hypothesize that the number of frozen days per year from passive microwave satellite data (SSM/I - Special Sensor Microwave Imager) can be used as indicator for permafrost extent. A 30 year record was analyzed for trends and compared to the map of Brown et al. (1997) - often referred to as the IPA (International Permafrost Association) map - and results of the CHANGE progress model (Park et al., 2011a). A threshold of half a year of frozen days during at least two consecutive years was chosen to delineate possible permafrost areas. This value was justified with reference to Dobinski (2011), Nelson and Outcalt (1987), Saito et al. (2013) and Zhang et al. (2005). These studies use measures derived from actual temperature records, specifically the use of mean annual air temperature and the concept of thawing/freezing degree days. Results showed differences between the model and microwave product, especially at the start of the record which could be due to sparse satellite data during the beginning of the chosen time period (Trofaier et al., 2017). The comparison with the IPA permafrost map revealed an overestimation of permafrost extent around 65°N. Overall, agreement regionally differed, especially over non-continuous permafrost. Luoto et al. (2004) suggest that the minimum number of frozen days is 200 for new permafrost to develop (in form of palsas) in the transition zone of Scandinavia. Additionally, local factors like a low annual mean temperature (<1°C), water-saturated peat, moss patches and low vegetation have to be present (Seppälä, 1986; Harris, 1981). This number is considerably higher, compared to the selection of Park et al. (2016).

Surface state information can be also derived from active microwave sensors operating at various frequencies (Park et al., 2011b; Naeimi et al., 2012; Bartsch et al., 2007; Wang et al., 2008; Zwieback et al., 2015) and with that the calculation of frozen and thawed days per year. Frequencies are usually lower than SSM/I and especially C-band (5.3 GHz) scatterometer like the ASCAT (Advanced Scatterometer) sensor on-board the Metop satellites have already been shown to be applicable for freeze-thaw information retrieval in permafrost regions by validation with near surface soil temperature from borehole records (Naeimi et al., 2012). Multi-annual statistics of thaw and freeze-up timing based on these records have been e.g. applied for the retrieval of circumpolar landscape units (Bartsch et al., 2016).

The number of frozen days can be observed consistently from space. Freezing degree days, as conventionally used, require spatial and temporal interpolation. The use of frozen days would therefore allow a purely observation based assessment. This does, however, require the assumption that the shape of the annual temperature curve can be represented by a sine (e.g. Frauenfeld et al., 2007) and changes at the surface (as represented by the satellite at a certain frequency) are uniformly and linearly related to sub-ground temperatures. This neglects effects such as insulation by snow as well as varying soil thermal conductivity. The validity of the approach may therefore be limited. In cases where it is applicable, it may, however, allow the estimation of actual ground temperatures and not only extent.

A further issue is the available data for calibration and validation of datasets spanning the entire Arctic. The map of Brown et al. (1997) does provide zones of permafrost occurrence which correspond to area fraction of permanently frozen ground. The actual patterns within the non-continuous zone are unknown, different sources have been used and it represents the stage of the second half of the 20th century. Results need to be therefore treated with care. It is however used in many studies for evaluation of modelling results (e.g. in Park et al., 2016; Matthes et al., 2017).

An alternative are actual ground temperature measurements. Borehole data represent, however, only point information, with uneven distribution (Biskaborn et al., 2015) and provide measurements at selected depths only. The mean annual ground temperature (MAGT) is currently only in same cases provided by the data owners within the Global Terrestrial Network on Permafrost (GTN-P) database. A practical method which allows use of all freely available data is required for circumpolar applications.

The objective of this study is to investigate the applicability of the frozen days approach based on satellite data for potential permafrost extend determination as well as MAGT retrieval. Special emphasis is given on suitability of calibration and validation data, differences between microwave sensors and uncertainties with respect to environmental conditions including snow, land cover and ground ice content. Regional patterns of agreement with the map of Brown et al. (1997) as well as with in situ data are discussed.

2 Datasets

2.1 Satellite records

We used two microwave remote sensing data sets derived from globally available records and with similar classification accuracy obtained by comparison to air temperature data. They are derived from sensors with different frequencies, acquisition

methods (active versus passive) and timing. The first was derived from the ASCAT sensor on-board the Metop satellites. The ASCAT sensor is a C-band (5.255 GHz) scatterometer (Figa-Saldaña, et al., 2002), providing almost daily coverage of the Earth's surface. The equator overpass time is 9:30 am. The surface state information (freeze/thaw) has been derived from the ASCAT sensor as a surface status flag for a soil moisture product specifically post-processed for high latitudes (Paulik et al.,

5 2014). The circumpolar data set covers the years 2007 - 2013. It was developed for permafrost monitoring and climate mod-elling purposes (Bartsch and Seifert, 2012; Naeimi et al., 2012; Reschke et al., 2012), and covers the area above 50°N with a grid spacing of 12.5 km and an up to daily temporal resolution (Paulik et al., 2014). This includes the parameters frozen and thawed ground, temporary water (including snow melt) and frozen water/permanent ice. The surface status information was derived using a step-wise threshold algorithm based on ASCAT backscatter values and ECMWF ReAnalyis data (Naeimi

10 et al., 2012). The accuracy was assessed with in situ surface air temperature measurements from the global weather station net-work and found to be about 82% overall (Naeimi et al., 2012). Up to 92% agreement was found for near surface temperature measurements from boreholes of GTN-P located in Siberia.

The second remotely sensed data set used in this study was derived from global daily (ascending and descending orbit) 37 GHz, vertically polarized brightness temperature observations from calibrated SMMR (scanning multi-channel microwave

15 radiometer) and SSM/I (special sensor microwave imager) satellite sensor records by Kim et al. (2014). There have been a series of those sensors carried on-board satellites from the Defense Meteorological Satellite Program. They are passive radio-metric systems that measure atmospheric, ocean and terrain microwave temperature (Hollinger et al., 1990). SSM/I equatorial crossings are 6 am and 6 pm. The freeze-thaw status was analyzed globally from 1979 - 2012 by Kim et al. (2014). The data set has a nominal resolution of 25 km and covers the Arctic terrestrial drainage basin. The actual footprint size at 37GHz is

20 37km x 28km. The threshold approach produces two classes: frozen and non-frozen. The estimated classification accuracy is approximately 85% (am passes) to 92% (pm passes) compared to in situ surface air temperature measurements from the global weather station network (Kim et al., 2012). This dataset has been used by Park et al. (2016) for the assessment of permafrost extent changes.

2.1.1 In situ records from boreholes

25 All borehole records above a latitude of 50° North with available time series of ground temperature were retrieved from the Global Terrestrial Network for Permafrost database (GTN-P, 2016). The network collects measurements of the Thermal State of Permafrost (TSP) in polar and mountain regions. 277 borehole sites have temperature data, single sites often comprise more then one measurement unit or period, which leads to a total sum of 1062 ground temperature data sets (Biskaborn et al., 2015). The depth of most boreholes is less than 25 m, although the average lies at 53 m. The most frequent sensor depth is found

30 at 5 m. Permanently installed multi-thermistor cables showing an accuracy between 0.002 - 0.1°C are most commonly used for measuring continuous ground temperatures at specific depths (Romanovsky et al., 2010). The time series are available in hourly, daily or annual resolution and cover different time periods. Deepest sensor depths of the used data set vary between 1m and 99m. In total 216 boreholes have been considered. They represent a Mean Annual Ground Temperature (MAGT) range from -15°C to 6°C. There are however inconsistencies in sensor spacing and the MAGT at zero annual temperature amplitude

is not directly measured. Most records of North America are accompanied with meta records which suggest es sensor depth for approximation of the MAGT. But this information is unavailable for the majority of records from Asia. MAGT together with the year which they represent has been available for 64 sites only (24% of all sites relevant for the analyses period).

2.1.2 Spatial information on environmental conditions

5 The circumpolar permafrost map by Brown et al. (1997) depicts the permafrost extent divided in different classes as well as the ground ice content for the Northern Hemisphere (20°N to 90°N). The data set defines permafrost as frozen ground that remains at or below 0°C for at least two years. Areas are classified as continuous, discontinuous, sporadic or isolated permafrost with differing ground ice content. The classes correspond to percent area categories: 90-100%, 50-90%, 10-50%, <10%, and no permafrost. These classes have been compared separately and as one aggregated class (excluding areas of no permafrost) to

10 the results of the frozen day classifications. Zones with specified ground ice content are also supplied with the permafrost map and used in this study. Classes are: high >20%, medium 10-20% and low <10%.

The Global Snow Monitoring for Climate Research (GlobSnow) dataset provides information about SWE and snow extent for the Northern Hemisphere (25°N - 84°N) (Metsämäki et al., 2015; GlobSnow). The products are based on Scanning Multichannel Microwave Radiometer (SMMR), Special Sensor Microwave Imager (SSM/I), and Advanced Microwave Scanning

15 Radiometer - Earth Observing System (AMSR-E) sensor data in combination with ground based measurements (GlobSnow; Takala et al., 2011). The SWE data product used in this study has a spatial resolution of 25km. The SWE values are provided as daily SWE, weekly aggregated SWE and monthly aggregated SWE. In this study, we used the monthly aggregated SWE which provides a maximum SWE value for each month to determine the maximum SWE for each winter.

The Global Land Cover 2000 Project (GLC 2000) provides global landcover information at 1km resolution (GLC2000,

20 2003). The data is mainly based on Satellite Pour l'Observation de la Terre-4 (SPOT-4) observations, partially supported by other Earth observing sensors (Bartholomé and Belward, 2005).

3 Methods

3.1 Preparation of borehole temperature data

The mean annual ground temperature (MAGT) is usually calculated at the depth of zero annual amplitude (ZAA) for permafrost

25 studies. As the availability of data at specific depths is limited, representing or reaching the depth of ZAA is not possible for all cases. The MAGT, defined as the temperature at a specific site in this study, was therefore calculated for each borehole location at the depth of the minimum MAGT. The minimum MAGT, in a stable climate, would be the same as the MAGT at the depth of ZAA (Bodri and Cermak, 2007). Where available, we have collected also meta data for all GTN-P boreholes regarding MAGT, the year of the calculation and depth of sensor representing MAGT in order to test the validity of this approach. Only sensors

30 with more than 1m depth have been used as the MAGT near the surface can be much colder than at larger depth. Temperature time series of the different sensors have been tested for gaps and inconsistencies. Only years with complete records have been

considered for calibration and validation. The used sites are located within an area with 150 to 330 number of frozen days as observed in the satellite records in order to account for artifacts which can occur due e.g. large water bodies within the footprint.

3.2 Pre-processing of satellite records

5 Both surface status data sets underwent post-processing before being used in our permafrost extent and temperature estimation. The ASCAT surface status flag (SSF) data contain cells with no data where the algorithm failed to produce a result. Gaps were filled by surrounding values (class with majority), ensuring a complete data set. The sum of frozen days per year for every pixel was determined for both satellite records, according to the method of Park et al. (2016). Grid cells where the number of frozen days exceeds the number of thawed days during two consecutive years are classified as permafrost. We have defined the 10 averaging period with respect to the water year from September 1 to August 31 as suggested by Park et al. (2016).

To explore the dependency of the results on snow melting events, the permafrost extent estimation from ASCAT data was carried out excluding the melt days in the count of frozen days (FT) and a second analysis counting the melt days as frozen grid cells (FM).

3.3 Frozen days threshold determination for potential permafrost extent

15 In the study of Park et al. (2016) a threshold of half a year was chosen for the delineation of permafrost extent. Half year corresponds to 180 or 182.5 days in climate models (Saito et al., 2013). In a first step, we extended the analysis to 210 frozen days to test the validity of the suggested threshold. The cross-comparison with the permafrost extent classes considers the information of four thresholds (180, 190, 200, 210) for the entire study area what allowed us to analyze the difference in estimated permafrost extent and the sensitivity of this approach to the chosen threshold. The results from both active and 20 passive microwave freeze/thaw data sets were compared with the permafrost map by Brown et al. (1997).

To evaluate the initial threshold of half a year with in situ data, ASCAT and SSM/I data were extracted for each of the borehole locations. We classified borehole (coldest sensor) derived MAGT > 0 as 0 and MAGT <= 0 as 1 and the DOY > "threshold" as 1 and DOY < "threshold" as 0. Kendall's Tau (τ) was used to examine the correlation coefficient between the in situ and satellite derived data set. It was chosen as it provides a method to measure the ordinal association to measured or 25 calculated quantities.

In order to determine the most suitable limit to map permafrost extent, thresholds where varied from 180 to 210 days in one day steps. For the evaluation of the initial threshold of 180 days we divided the dataset (all years and stations) into four sectors; positive and negative MAGT versus DOY >= 180 and DOY < 180. The number of considered data points differ between SSM/I and ASCAT due to different masking schemes.

30 The classified maps (initial half year threshold) have been summed up for each data type for the four periods to obtain information on interannual and spatial variability. ASCAT FT and SSM/I results have been compared by deriving the difference between the individual sums.

3.4 Model parameterization for potential mean annual ground temperature retrieval

The relationship between MAGT and frozen day of year was further examined for the retrieval of ground temperature and consecutive determination of permafrost extent by using the 0°C threshold. Only data inside the range of 150 to 330 frozen DOY have been considered. Additionally, sites which are located on islands in the high Arctic have been excluded with respect to microwave sensor footprint size. The remaining 168 sites haven been used to fit the model. The records from ASCAT as well as SSM/I have been split into two parts by defining a calibration (2009-2011) and a validation period (2007-2008). We tested linear, logarithmic and polynomial functions on their ability to describe the relationship between MAGT and day of year frozen. We found no significant fit for polynomial functions and a slightly weaker fit for logarithmic functions compared to a simple linear regression. Therefore a linear model has been applied to the frozen days for the years 2009 to 2011 for the determination of an empirical relationship. The resulting formula was used to estimate the MAGT from the day of year data set for the years 2007 and 2008. The differences between the modelled and in situ MAGT have been calculated separately for the two years in order to assess the capability of the approach to capture inter-annual variations, to investigate various environmental impacts (snow water equivalent, landcover type), differences between previously defined permafrost zones and specific regions. The Arctic has been split up into 12 regions in the latter case (Fig. A1).

The average MAGT for the entire time period (2007-2011) has been calculated for ASCAT FT and SSM/I results and compared. The standard deviation has been derived in addition.

The MAGT values have been eventually classified for each year in order obtain permafrost extent maps (binary maps of values below and above zero degree Celsius). They have been summed up for each data type for the four periods to obtain information on interannual variability. ASCAT FT and SSM/I results have been compared similarly as for the test of the initial threshold (see section 3.3).

4 Results

4.1 Evaluation of in situ MAGT at coldest sensor depth

64 borehole locations had meta data suitable for the assessment. 20 of the boreholes belong to the Vorkuta GTN-P site. R^2 between MAGT meta records and at coldest sensor depth 0.994 (Fig. 1). The RMSE is 0.38 °C. Derived values tend to be colder by on average 0.2 °C. The coldest sensor depth and sensor to be used agreed in 58 (90%) of the samples. Deviations of sensor depth occurred only for the Alaskan sites Bonanza Creek and Atmautluak as well as Arctic Bay (Nunavut Canada), Kursflaket 2 (Sweden), Ishim (Tyumen, Russia) and Kotkino (Western Russia), however, with only little deviations in MAGT. They have been below 0.1°C except for Bonanza Creek (-0.39°C). MAGT at cold sensor depth seems to be also valid in non-permafrost regions based on the available records.

4.2 Threshold sensitivity analyses and permafrost extent

The area mapped as permafrost with a frozen day threshold of 180 days for the period 2007-2011 differs regionally between the ASCAT and the SSM/I data set (Fig. 2). The extent of areas where only ASCAT determines permafrost is about four times higher than for SSM/I. The latter largely occurs outside the expected permafrost extent. Deviations in the transition zone

5   are low for Western Siberia but still present. The classification using SSM/I data results in a smaller permafrost extent for the Canadian Arctic compared to Brown et al. (1997). Most of the transition zone (including sporadic and isolated) in this region has more than 180 days frozen in the ASCAT dataset. The Canadian High Arctic is also largely not covered by the SSM/I dataset. ASCAT overestimates the permafrost extent in Scandinavia. In general high latitudinal lowland permafrost is overestimated with ASCAT whereas the extent in more southern uplands and mountain regions is overestimated with SSM/I

10 using the initial threshold.

Mapped permafrost extent varies for each threshold step across the different zones. The largest deviation in area extent for continuous permafrost occurs in the SSM/I result with more than 2.5 Mio km^2 lower values than in Brown et al. (1997) (more than 12 %, Tab. 3). Less than 1 Mio km^2 (less than 5% of total continuous permafrost area) is missed by ASCAT. This applies to thresholds between 180 and 200 frozen days (excluding snow melt days). Matching extent is lowest for 200 days in case

15 of inclusion of snow melt days. ASCAT maps more permafrost outside the boundaries of Brown et al. (2007) than SSM/I in case of a 180 day threshold but agrees better than SSM/I for discontinuous and isolated permafrost area. This results in lower percentage agreement of the SSM/I product for the total permafrost extent (Tab. 4). The false permafrost detection by ASCAT is out-weighted by a significantly higher detection performance for the total extent. There is also more year to year variability in the results from the analysis using SSM/I data than from ASCAT.

20 ## 4.3 Determination of optimal threshold with Kendall's τ test and in situ measurements

The comparison of the satellite records with in situ data demonstrates differences between the datasets. For the ASCAT data sets the best τ was found to coincide with 204 (FM) and 203 (FT) frozen DOY (Tab. 2), whereas for the SSM/I 190 DOY showed the highest τ with a steep gradient before and after the peak (Fig. 3).

With the DOY threshold of 180 days, the algorithm tends to overestimate the amount of negative MAGT values, while the

25 threshold found by the Kendall's τ leads to an underestimation of negative MAGT values below the threshold. (Tab. 1). It is highest for exclusion of snow melting days. On the other hand the ASCAT results show nearly no negative MAGT below the threshold of 180. The thresholds delineated by the best correlation coefficient (Kendall's τ) indicate for all data sets a better performance regarding positive MAGT in areas below the threshold. However, the higher thresholds lead also to more negative MAGT in these areas. For the SSM/I 75% of MAGT temperatures can be correctly allocated with both thresholds. The ASCAT

30 results show a higher accuracy with more than 80% correctly assigned values.

ASCAT and SSM/I maps derived with the initial threshold of 180 days mostly agree in the continuous permafrost zones over the four analyses periods (Fig. 2). ASCAT overestimates permafrost extent in Northern America, Scandinavia and Western Siberia. SSM/I overestimates specifically in southern Central Siberia.

Table 1. Comparison matrix between in situ Mean Annual Ground Temperature (MAGT, at coldest sensor depth) classes (below or above zero °C) and classified number of frozen days per year from ASCAT (FT - excluding snow melt days, FM - including snow melt days) and SSM/I for 2007-2012. Both, the initial 180 Days of Year (DOY) threshold and the optimal threshold based on best Kendall's τ are assessed. Values represent numbers of sites for multiple years. Rows indicating false classifications are in *italic*.

Sensor	ASCAT FT		ASCAT FM		SSM/I	
DOY	**180**	**203**	**180**	**204**	**180**	**190**
Positive MAGT & DOY <thres.	142	211	127	199	115	148
Negative MAGT & DOY <thresh.	*2*	*70*	*0*	*35*	*14*	*41*
Positive MAGT & DOY >= thresh.	*138*	*69*	*153*	*81*	*157*	*124*
Negative MAGT & DOY >= thresh.	494	426	496	461	398	371
Sum of data points	776	776	776	776	684	684

Table 2. Comparison between in situ Mean Annual Ground Temperature (MAGT, at coldest sensor depth) with number of frozen days per year from ASCAT (FT - excluding snow melt days, FM - including snow melt days) and SSM/I for 2007-2012.

Parameter	ASCAT FT	ASCAT FM	SSM/I
Pearson correlation for linear fit	0.66	0.64	0.39
RMSE validation years (2007/2008)	2.15	2.21	2.53
RMSE all years (2007 - 2011)	2.22	2.24	2.57
DOY for zero degree C from linear fit	207	212	205
DOY for best Kendall's τ	203	204	190

4.4 Mean annual ground temperature determination for retrieval of permafrost extent

The classification of the derived MAGT dataset provides different results than the other methods. The DOY for intersection of the derived linear function at zero degree C corresponds to a higher number of frozen days in all cases (Tab. 2). The Pearson correlation for the linear fit decreases slightly from 0.66 to 0.64 if snow melting days are included (Fig. 4 and Tab. 2). The same applies to the residual standard error (2.15 versus 2.21) for the validation years. The slope of the linear fit also differs slightly between the two ASCAT data sets (Fig. 4). It is steeper in case of exclusion of melting days as well as for SSM/I. The spread of in situ temperature values is higher for conditions below 0°C than above. This is similar for all data sets. The majority of MAGT values (in a wide range of -10°C to 5°C) are found in the sector between 170 and 250 frozen DOY for ASCAT. The Pearson correlation in case of SSM/I is lower with 0.39 and RMSE is higher with 2.53°C (Fig. 4). A difference of 11 frozen days of near surface soil corresponds to 1°C in case of ASCAT FT.

The number of years which have MAGT below zero degree Celsius are similar between ASCAT (FT) and SSM/I in the lowland continuous permafrost zones (Fig. 2). Deviations are high in transition zones, especially southern Central Siberia, with a similar spatial pattern as observed already in the case of initial threshold comparison (Fig. 5). The results deviate by four

periods in this region, meaning that SSM/I always remains below a MAGT below zero degree Celsius, and ASCAT in none of the periods.

Deviations in derived potential MAGT between ASCAT and SSM/I occur within and outside the continuous permafrost region (Fig. 6). Larger differences occur over mountain ranges and lake rich areas. The results based on SSM/I are mostly warmer in the continuous zone. The temperature difference between ASCAT (FT) and SSM/I exceeds two degree Celsius in the Central Siberian transition zone, where SSM/I retrievals result in colder MAGT than for ASCAT.

The FT and FM methods differ more for the year 2007 than for 2008 (Fig. 7 and Tab. 5). The SSM/I extent misses a large proportion of continuous permafrost and maps additional area as permafrost (more pronounced in 2007, Tab. 5), similarly to the initial threshold based comparison to the permafrost extent map (Tab. 3).

4.4.1 Evaluation with in situ data with respect to region

The regionally averaged difference is mostly below one degree Celsius for all three products (Fig. 8). The deviations of ASCAT results from in situ records differ for most regions also between the two validation years. Large differences occur specifically in Western Russia and across Siberia for ASCAT FM as well as SSM/I. The exclusion of snow melting days reduces these differences. The deviations of the SSM/I product are largest in central Russia and the Jakutsk region. This is consistent with the patterns observed in comparison to the permafrost map (Fig. 5) and the deviations between the permafrost extent maps (Fig. 2 and Fig. 9).

The inclusion of days with melting snow reduces the deviations in Sweden, Jamal-Nenets district and West Russia, but increases for the Canadan Arctic Alaska (Fig. 8). The model result for ASCAT FM is about two degree colder than what is obtained from the in situ records in the first case. The spread is lowest for the Jakutsk region in case of ASCAT (Fig. 10). Median values are in general similar between inclusion and exclusion of melting snow.

4.4.2 Evaluation with in situ data with respect to environmental conditions

Deviations of MAGT are larger at sites with SWE larger than 150 mm (Fig. 11). Model results are colder than retrievals from the in situ records. This applies also for exclusion of the snow melting period. However, the exclusion reduces deviations in all medium SWE classes. Sites with high SWE are mostly located in Western Russia (Vorkuta region, Bolvansky) and Western Siberia (Nadym region, Urengoy).

The regions identified as sporadic and isolated permafrost in Brown et al. (1997) show comparably large offsets (Fig. 11). The isolated class does however only includes five samples. The exclusion of snowmelt specifically reduces the deviations in the discontinuous zone. In case of the ASCAT products, average deviation is always below 1°C in the continuous permafrost zone. The exclusion of melting snow clearly reduces deviations in case of high ground ice content.

Figure 12 shows results for different landcover classes.This seems to result in higher deviations for specifically the SSM/I results. Only two samples were available in the burned area class. The model results are warmer in both cases. Sites which are contained in the water class are located in proximity to larger lakes or ocean.

4.5 Comparison between permafrost extent maps

The results from all three tested methods for potential permafrost determination (half year threshold, best Kendall's τ and from modelled MAGT) are shown in Fig. 5. The largest spatial differences between included/excluded melting days occur in the same regions (Northeastern Canada and Scandinavia), which show the largest differences between the ASCAT and SSM/I 180 day threshold maps. An additional region of disagreement is Jakutsk. The inclusion of snow melting days leads here to a reduction of permafrost extent which is contradictory to most other regions.

The modelled extent and best Kendall's τ threshold results includes the discontinuous permafrost zone in Northern America for ASCAT (Fig. 5). The exclusion of melting snow has a large impact over Scandinavia. It leads to results which are more similar to the map of Brown et al. (1997). It is also one of the regions with extensive snow melt detected by ASCAT (Fig. A2). Patterns of continuous permafrost boundaries in central Asia (e.g. region around lake Baikal) are better represented in the ASCAT maps than in the SSM/I retrievals.

Variation of potential MAGT from year to year are much larger for SSM/I. Standard deviation is comparably high for the transition zone in Western Siberia and also the Canadian Arctic (Fig. 13). This pattern agrees with results obtained with the initial threshold in comparison to Brown et al. (1997) (see Section 4.2).

5 Discussion

5.1 General issues

The overall performance of permafrost extent mapping using number of frozen days is limited but reveals regional patterns in uncertainties. The extent of permafrost estimated with the initial threshold is in the order of the actual extent but the error of commission is relatively large. This problem can be tackled by adjustment of the threshold and use of different type of satellite acquisitions (ASCAT versus SSM/I). The performance of the empirical model for MAGT (based on coldest sensor, Tab. 2) is partially lower than what can be achieved with the more complex TTOP model (Westermann et al., 2015) which considers terrain, snow, land cover and land surface temperature measurements from satellite data. Westermann et al. (2015) reported a model accuracy of 2.5°C. Permafrost temperatures are also not always representing current climate conditions (Lachembruch and Marshall, 1986). This may regionally impact the comparability of the borehole records with surface observations. Estimates of permafrost temperatures as well as extent are therefore providing a potential distribution only. Results may however support the identification of regions where permafrost extent maps, including continuity classes, need to be treated with care. This includes Western and Central Siberia.

The mean annual ground temperature from boreholes was calculated from the coldest sensor below 1 m. The depth of these sensors varies from borehole to borehole what may impact the empirical model representativity. A high number of sites has been however chosen for calibration what may weaken the impact. The evaluation results with MAGT in the meta records for 24% of the sites support the assumption that the sensor at coldest depth can be used for approximation. Uncertainties introduced by variable sensor spacing can, however, not be addressed with the available data.

The in all cases (ASCAT and SSM/I, for all methods) higher accounts of number of frozen days than the previously suggested half year threshold agrees with field observations by Luoto et al. (2004), who estimated a minimum number of 200 days for permafrost formation for Scandinavia. 200 days corresponds to approximately 0.5°C in case of ASCAT FT. Considering local factors such as water-saturated peat and organic layer and uncertainties in the retrieval (difference to actual mean temperature),

5   this might still be counted as sufficient for permafrost formation. Variations of topography within the footprint lead also to local deviations from days to weeks (Bergstedt and Bartsch, 2017). We therefore suggest the consideration of temperature buffers when such data are applied. Boreholes with in situ MAGT below 0°C located in these buffer zones may represent sites where local factors are important. The role of past climate conditions for present ground temperatures need to be considered in addition. Location specific soil and snow properties may also need to be considered (see Section 5.4).

10   The classes in Brown et al. (1997) correspond to area fraction of permanently frozen ground. In case of the isolated permafrost class it can be assumed that at least 10% are below 0°C, but the actual mean temperature for a region in these areas (as e.g. represented by an ASCAT or SSM/I cell) can be below or above 0°C depending on local parameters such as topography and soil properties which impact thermal conductivity. The latter especially plays a role for occurrence of permafrost in the transition zone. Higher spatial resolution data sets would be required. Relevant measurements from microwave data are only

15   available from active systems due to technical constraints. Synthetic Aperture Radar (SAR) instruments could be used in case of sufficient sampling intervals (Park et al., 2011b). Current systems and acquisition plans do however not provide a sufficient sampling, temporally and spatially (Bartsch et al., 2016).

5.2   Regional issues

A threshold higher than the previously suggested half year leads to better performance of ASCAT than for SSM/I especially

20   over Scandinavia, west of the Ural Mountains and Eastern Russia (Chabarovsk region) (Fig. 5). ASCAT better captures the regional patterns as in Brown et al. (1997) with the exception of Scandinavia. The actual temperature amplitude (freezing and thawing degree days) may need to be considered in this region. The longer snow melt period (Fig. A2) also indicates a certain amount of snow which may lead to decoupling of air and ground temperatures.

The highest density of boreholes with available data is in the Vorkuta region in Western Russia. This region shows the largest

25   sensitivity to inclusion/exclusion of snow melting days. Here, the ASCAT results differ by more than two degree Celsius (lower temperature). This might have an impact on the average deviation derived from the entire borehole records. It is likely larger for the ASCAT FM result than calculated as most other regions show better agreement.

The majority of boreholes located in the regions 'Central Russia' and 'Central Siberia' show higher than zero degree MAGT (Fig. 8 and Fig. 10). The validation results differ from those of the other areas. SSM/I results suggest between one to two

30   degree lower regionally averaged MAGT values.

The Greenland and Svalbard sites are expected to have the highest variations due to the mixture of glaciers, land area and ocean within the ASCAT as well as SSM/I pixels. There is actually no coverage of the Greenland sites in the SSM/I records.

5.3 Performance differences between ASCAT and SSM/I

Results suggest that SSM/I freeze/thaw records are less suitable to derive actual MAGT values below zero degree Celsius (Fig. 6). The thresholds obtained for SSM/I are considerably lower than for ASCAT, what might be the result of the different wavelength, the sensing technique (passive/active), overpass timing and classification methods used to create these data sets.

The considerable lower number of frozen days in regions with low MAGT might be the result of the retrieval method (treatment regarding acquisition timing) and sensitivity to soil state changes. The instruments also differ in wavelength apart from the fact that one is active and the other passive. ASCAT uses C-band with about 5.7 cm and the SSM/I channel used by Park et al. (2016) about 0.8 cm. This results in different signal interactions with objects on the earth surface including snow and vegetation. It can be expected that the C-band signal is less sensitive to interactions, although present. The latter issue could be addressed by L-band missions with even lower frequency than ASCAT such as SMOS (Soil Moisture and Ocean Salinity Mission) or SMAP (Soil Moisture Active and Passive). In general, the role of acquisition timing and sampling rate needs to be investigated in more detail for permafrost related applications for ASCAT as well as SSM/I.

The lower performance of SSM/I might be also attributed to the fact that it has an even larger footprint (although gridded to 25km) than ASCAT. The validation results are therefore not fully comparable between the sensors for the entire Arctic, only on regional level. This may also affect the calibration, since the number of available samples is lower for SSM/I. It affects especially colder sites (Fig. 4). In general, less areas are masked in the ASCAT product. This applies to especially lake rich regions (Fig. 5). Findings of Bergstedt and Bartsch (2017) suggest an offset of the state change in the resolution cell due to lakes. This may lead to lower accuracy in these regions.

5.4 The role of environmental conditions

The amount of snow seems to play the most important role for the applicability of the frozen day approach. One may expect warmer modelled MAGT than in situ values in transitions zones due to the fact that boreholes in transition zones often represent isolated patches of permafrost. However, the opposite is the case (Fig. 11), what may relate to the importance of the insulation effect of snow cover in these regions, e.g. as known for Skandinavia (Luoto et al., 2004). Landcover seems to be of minor importance it only plays a role when comparing performance of SSM/I versus ASCAT.

The number of snow melting days are in general highly variable in the Arctic (Bartsch, 2010) but the melting period is comparably short (Zhang et al., 2005). Snowmelt is expected to delay the soil surface warming due to latent heat and therefore cools the soils (Zhang et al., 2005). Latent heat released due to refreeze of meltwater may have a warming effect after a few days (Dingman et al., 1980). Dingman et al. (1980) also report start of soil thaw before the end of snowmelt at Barrow. The overall impact of snowmelt is expected to be dependent on local conditions (Zhang et al., 2005). Our results suggest that there is a warming effect with an impact on MAGT. Days with melting snow should be therefore treated as unfrozen. This leads to higher MAGT (on average 1°C for considered borehole locations) and better agreement with in situ measurements. Exclusion of the snowmelt period is also consistent with calculation of thawing and freezing degree days from air temperature data. The snowmelt period does also count as unfrozen in this case.

Snow melting days are, however, not mapped for all grid points in case of the ASCAT data set (Fig. A2). This may depend on snow depth as well as acquisition timing. The coverage pattern is irregular across the Arctic with a mix of morning and evening (ascending and descending orbits) measurements (Bergstedt and Bartsch, 2017). Usually only evening measurements capture the melt as diurnal freeze and thaw cycles are common (Bartsch et al., 2007). The differentiation between frozen and
5 melting days may however be valid in regions with prolonged melt and high SWE. Areas with melting snow in the ASCAT data set are common in the high Arctic, in areas with low MAGT (Fig. A2) as well as areas in the transitions zone (such as Scandinavia). This pattern differs from the length of the snow melt period detected with Seawinds QuikScat, a Ku-band scatterometer (Bartsch, 2010), which provides several measurements per day. The number of days with snow melt are much lower in C-band than in the Ku-band product. This could be attributed to the lower sensitivity of C-band to melting processes
10 and the limited temporal sampling. In addition, the QuikScat results in Bartsch (2010) are representing periods of freezing and thawing which can contain breaks (with frozen conditions) of up to ten days.

6 Conclusions

The low differences between the tested methods within the continuous permafrost zone (as defined in Brown et al. (1997)) indicate low uncertainties for these regions. Exceptions are mountain ranges. Deviations in transition areas are largest in
15 southern Central Siberia and areas with high snow depth. This underlines the importance of snow and suggests that advanced models should be applied in the areas of the mountain ranges in central Asia, including central Jakutia and Mongolia.

The direct comparison of the number of frozen days to MAGT reveals the potential of C-band scatterometer based surface status detection for ground temperature mapping. A linear empirical model and exclusion of melting snow provide the best results when compared to MAGT at coldest sensor depth.
20 All four approaches for utilization of satellite derived surface state point to a higher number of frozen days threshold than 180 days for the determination of permafrost extent: (1) the quantification of area overlap with the permafrost map by Brown et al. (1997), (2) Kendall's τ test using borehole measurements (Fig. 3), (3) in situ data matrix using borehole measurements (Table 1) as well as (4) the direct comparison to in situ MAGT at coldest sensor depth (Table 2). This applies not only to the ASCAT data but also to the SSM/I data for which a half year threshold has been initially proposed.
25 The direct comparison to borehole temperatures reveals the potential of C-band scatterometer based surface status detection for ground temperature estimation. A linear empirical model performs with an RMSE of less than 2.2 °C when days with melting snow are excluded. The modelled temperature deviates on average by less than one degree Celsius in footprints without glaciers and mix of land and water. Especially regions with large variations of frozen days between the years and/or between the three different products (ASCAT with snow melting days and without, the SSM/I records) need to be further investigated with
30 respect to the representativity of the borehole records and derived temperatures respectively (e.g. Western Siberia). They mostly correspond to the permafrost transition zones. The validity of the coarse resolution microwave satellite records for the point locations needs to be confirmed by e.g. using higher spatial resolution synthetic aperture radar (SAR) records. More detailed analyses of the role of melting snow conditions is required in addition. Conventional approaches for spatially continuous

mapping of permafrost temperatures require gap filling or spatial interpolation. The C-band radar record provides a purely observational account.

7 Data availability

The average annual sums of frozen and snow melting days derived from Metop ASCAT are available via the ESA DUE GlobPermafrost project WebGIS and catalogue. www.globpermafrost.info.

Author contributions. CK has performed all data analyses and contributed to the preparation of figures. The concept of the paper was jointly developed by CK and AB. AB wrote the majority of manuscript. CK contributed to the writing of the in situ, methods and results sections, HB to the satellite data description and discussion.

Competing interests. The authors declare no conflict of interest

Acknowledgements. This work was supported by the Austrian Science Fund (Fonds zur Förderung der wissenschaftlichen Forschung, FWF) under Grant [I 1401] (Joint Russian–Austrian project COLD-Yamal), Grant [DK W1237-N23] (Doctoral College GIScience) as well as the European Space Agency project DUE GlobPermafrost (contract number 4000116196/15/I-NB).

References

André, C., Ottlé, C., Royer, A., and Maignan, F.: Land surface temperature retrieval over circumpolar Arctic using SSM/I–SSMIS and MODIS data, Remote Sensing of Environment, 162, 1 – 10, doi:10.1016/j.rse.2015.01.028, 2015.

Bartholomé, E. and Belward, A. S.: GLC2000: a new approach to global land cover mapping from Earth observation data, International Journal of Remote Sensing, 26, 1959–1977, doi:10.1080/01431160412331291297, https://doi.org/10.1080/01431160412331291297, 2005.

Bartsch, A.: Ten Years of SeaWinds on QuikSCAT for Snow Applications, Remote Sensing, 2, 1142–1156, doi:10.3390/rs2041142, 2010.

Bartsch, A. and Seifert, F. M.: The ESA DUE Permafrost project - A service for high latitude research, in: 2012 IEEE International Geoscience and Remote Sensing Symposium, pp. 5222–5225, doi:10.1109/IGARSS.2012.6352432, 2012.

Bartsch, A., Kidd, R. A., Wagner, W., and Bartalis, Z.: Temporal and Spatial Variability of the Beginning and End of Daily Spring Freeze/Thaw Cycles Derived from Scatterometer Data, Remote Sensing of Environment, 106, 360–374, doi:10.1016/j.rse.2006.09.004, 2007.

Bartsch, A., Höfler, A., Kroisleitner, C., and Trofaier, A. M.: Land Cover Mapping in Northern High Latitude Permafrost Regions with Satellite Data: Achievements and Remaining Challenges, Remote Sensing, 8, 979, doi:10.3390/rs8120979, 2016.

Bartsch, A., Kroisleitner, C., and Heim, B.: Circumpolar Landscape Units, links to GeoTIFFs, doi:10.1594/PANGAEA.864508, https://doi.pangaea.de/10.1594/PANGAEA.864508, supplement to: Bartsch, A et al. (2016): An Assessment of Permafrost Long-term monitoring sites with circumpolar satellite derived datasets. Proceedings of the ESA Living Planet Symposium 2016. ESA SP-740, Prague, Czech Republic, 6 pp, hdl:10013/epic.48548.d001, 2016.

Bergstedt, H. and Bartsch, A.: Surface State across Scales; Temporal and SpatialPatterns in Land Surface Freeze/Thaw Dynamics, Geosciences, 7, 65, doi:10.3390/geosciences7030065, 2017.

Biskaborn, B. K., Lanckman, J.-P., Lantuit, H., Elger, K., Streletskiy, D. A., Cable, W. L., and Romanovsky, V. E.: The new database of the Global Terrestrial Network for Permafrost (GTN-P), Earth System Science Data, 7, 245–259, doi:10.5194/essd-7-245-2015, 2015.

Bodri, L. and Cermak, V.: Borehole CLimatology: a new method how to reconstruct climate, Elsevier Science, 1st edn., 2007.

Brown, J., Ferrians, Jr., O., Heginbottom, J., and Melnikov, E.: Circum-Arctic map of permafrost and ground-ice conditions, 1997.

Brown, R., Derksen, C., and Wang, L.: Assessment of Spring Snow Cover Duration Variability over Northern Canada From Satellite Dataset, Remote Sensing of Environment, 111, 367–381, 2007.

Cheng, G. and Wu, T.: Responses of permafrost to climate change and their environmental significance, Qinghai-Tibet Plateau, Journal of Geophysical Research: Earth Surface, 112, doi:10.1029/2006JF000631, 2007.

Dingman, S., Barry, R., Weller, G., C.Benson, LeDrew, E., and Goodwin, C.: Climate, Snow Cover, Microclimate, and Hydrology, in: An Arctic Ecosystem: the Coastal Tundra at Barrow, edited by Brown, J., Miller, P., and Bunnell, F., chap. 2, pp. 30–65, Hutchinson and Ross, Stroudsburg, PA, 1980.

Dobinski, W.: Permafrost, Earth-Science Reviews, 108, 158 – 169, doi:10.1016/j.earscirev.2011.06.007, 2011.

Figa-Saldaña,, J., Wilson, J., Attema, E., Gelsthorpe, R., Drinkwater, M., and Stoffelen, A.: The advanced scatterometer (ASCAT) on the meteorological operational (MetOp) platform: A follow on for European wind scatterometers, Canadian Journal of Remote Sensing, 28, 404–412, doi:10.5589/m02-035, 2002.

Frauenfeld, O. W., Zhang, T., and Mccreight, J. L.: Northern Hemisphere freezing/thawing index variations over the twentieth century, International Journal of Climatology, 27, 47–63, doi:10.1002/joc.1372, http:https://doi.org/10.1002/joc.1372, 2007.

GLC2000: The Global Land Cover Map for the Year 2000, european Commision Joint Research Centre, http://www-gem.jrc.it/glc2000. Access date: 12/01/2017, 2003.

GlobSnow: Global Snow Monitoring for Climate Research, http://www.globsnow.info.Accessdate:12/01/2017.

Gruber, S.: Derivation and analysis of a high-resolution estimate of global permafrost zonation, The Cryosphere, 6, 221–233, doi:10.5194/tc-6-221-2012, 2012.

GTN-P: Global Terrestrial Network for Permafrost Database: Permafrost Temperature Data (TSP Thermal State of Permafrost), 2016.

Harris, S. A.: Distribution of zonal permafrost landforms with freezing and thawing indices, Erdkunde, 35, 81–90, doi:10.3112/erdkunde.1981.02.01, 1981.

Hayes, D. J., Kicklighter, D. W., McGuire, A. D., Chen, M., Zhuang, Q., Yuan, F., Melillo, J. M., and Wullschleger, S. D.: The impacts of recent permafrost thaw on land–atmosphere greenhouse gas exchange, Environmental Research Letters, 9, 045 005, 2014.

Hollinger, J. P., Peirce, J. L., and Poe, G. A.: SSM/I instrument evaluation, IEEE Transactions on Geoscience and Remote Sensing, 28, 781–790, doi:10.1109/36.58964, 1990.

Kim, Y., Kimball, J. S., Zhang, K., and McDonald, K. C.: Satellite detection of increasing Northern Hemisphere non-frozen seasons from 1979 to 2008: Implications for regional vegetation growth, Remote Sensing of Environment, 121, 472–487, 2012.

Kim, Y., Kimball, J. S., Glassy, J., and McDonald, K. C.: MEaSUREs Global Record of Daily Landscape Freeze/Thaw Status, Version 3, doi:10.5067/MEASURES/CRYOSPHERE/nsidc-0477.003, 2014.

Lachembruch, A. H. and Marshall, B. V.: Changing climate: geothermal evidence from permafrost in the Alaskan Arctic, Science, 234, 689 – 696, 1986.

Luoto, M., Fronzek, S., and Zuidhoff, F. S.: Spatial modelling of palsa mires in relation to climate in northern Europe, Earth Surface Processes and Landforms, 29, 1373–1387, doi:10.1002/esp.1099, 2004.

Matthes, H., Rinke, A., Zhou, X., and Dethloff, K.: Uncertainties in coupled regional Arctic climate simulations associated with the used land surface model, Journal of Geophysical Research: Atmospheres, 122, 7755–7771, doi:10.1002/2016JD026213, http://dx.doi.org/10.1002/2016JD026213, 2016JD026213, 2017.

Metsämäki, S., Pulliainen, J., Salminen, M., Luojus, K., Wiesmann, A., Solberg, R., Böttcher, K., Hiltunen, M., and Ripper, E.: Introduction to GlobSnow Snow Extent products with considerations for accuracy assessment, Remote Sensing of Environment, 156, 96 – 108, doi:https://doi.org/10.1016/j.rse.2014.09.018, http://www.sciencedirect.com/science/article/pii/S0034425714003630, 2015.

Naeimi, V., Paulik, C., Bartsch, A., Wagner, W., Kidd, R., Boike, J., and Elger, K.: ASCAT Surface State Flag (SSF): Extracting Information on Surface Freeze/Thaw Conditions from Backscatter Data Using an Empirical Threshold-Analysis Algorithm, IEEE Transactions on Geoscience and Remote Sensing, 50, 2566–2582, doi:10.1109/TGRS.2011.2177667, 2012.

National research Council: Abrupt impacts of climate change: Anticipating surprises, National Academies Press, 2013.

Nelson, F. E. and Outcalt, S. I.: A Computational Method for Prediction and Regionalization of Permafrost, Arctic and Alpine Research, 19, 279–288, 1987.

Nguyen, T., Burn, C., King, D., and Smith, S.: Estimating the extent of near surface permafrost using remote sensing, Mackenzie Delta, Northwest Territories, Permafrost and Periglacial Processes, 20, 141–153, doi:10.1002/ppp.637, 2009.

O'Connor, F. M., Boucher, O., Gedney, N., Jones, C. D., Folberth, G. A., Coppell, R., Friedlingstein, P., Collins, W. J., Chappellaz, J., Ridley, J., and Johnson, C. E.: Possible role of wetlands, permafrost, and methane hydrates in the methane cycle under future climate change: A review, Reviews of Geophysics, 48, n/a–n/a, doi:10.1029/2010RG000326, rG4005, 2010.

O'Donnell, J. A., Jorgenson, M. T., Harden, J. W., McGuire, A. D., Kanevskiy, M. Z., and Wickland, K. P.: The Effects of Permafrost Thaw on Soil Hydrologic, Thermal, and Carbon Dynamics in an Alaskan Peatland, Ecosystems, 15, 213–229, doi:10.1007/s10021-011-9504-0, 2012.

Park, H., Iijima, Y., Yabuki, H., Ohta, T., Walsh, J., Kodama, Y., and Ohata, T.: The application of a coupled hydrological and biogeochemical model (CHANGE) for modeling of energy, water, and CO2 exchanges over a larch forest in eastern Siberia, Journal of Geophysical Research: Atmospheres, 116, doi:10.1029/2010JD015386, d15102, 2011a.

Park, H., Kim, Y., and Kimball, J.: Widespread permafrost vulnerability and soil active layer increases over the high northern latitudes inferred from satellite remote sensing and process model assessments, Remote Sensing of Environment, pp. 349–358, doi:10.1016/j.rse.2015.12.046, 2016.

Park, S.-E., Bartsch, A., Sabel, D., Wagner, W., Naeimi, V., and Yamaguchi, Y.: Monitoring Freeze/Thaw Cycles Using ENVISAT ASAR Global Mode, Remote Sensing of Environment, 115, 3457–3467, 2011b.

Paulik, C., Melzer, T., Hahn, S., Bartsch, A., Heim, B., Elger, K., and Wagner, W.: Circumpolar surface soil moisture and freeze/thaw surface status remote sensing products (version 4) with links to geotiff images and NetCDF files (2007-01 to 2013-12), doi:10.1594/PANGAEA.832153, https://doi.pangaea.de/10.1594/PANGAEA.832153, 2014.

Reschke, J., Bartsch, A., Schlaffer, S., and Schepaschenko, D.: Capability of C-Band SAR for Operational Wetland Monitoring at High Latitudes, Remote Sensing, 4, 2923–2943, 2012.

Romanovsky, V., Smith, S., and Christiansen, H.: Permafrost Thermal State in the Polar Northern Hemisphere during the International Polar Year 2007-2009: a Synthesis, Permafrost and Periglac. Process., 21, 106–116, doi:10.1002/ppp.689, 2010.

Saito, K., Sueyoshi, T., Marchenko, S., Romanovsky, V., Otto-Bliesner, B., Walsh, J., Bigelow, N., Hendricks, A., and Yoshikawa, K.: LGM permafrost distribution: how well can the latest PMIP multi-model ensembles perform reconstruction?, Climate of the Past, 9, 1697–1714, doi:10.5194/cp-9-1697-2013, 2013.

Schuur, E., Bockheim, J., Canadell, J., and Euskirchen, E.: Vulnerability of permafrost carbon to climate change: Implications for the global carbon cycle, BioScience, doi:10.1641/B580807, 2008.

Schuur, E. A. G., McGuire, A. D., Schädel, C., Grosse, G., Harden, J. W., Hayes, D. J., Hugelius, G., Koven, C. D., Kuhry, P., Lawrence, D. M., Natali, S. M., Olefeldt, D., Romanovsky, V. E., Schaefer, K., Turetsky, M. R., Treat, C. C., and Vonk, J. E.: Climate change and the permafrost carbon feedback, Nature, 520, 171–179, doi:10.1038/nature14338, 2015.

Seppälä, M.: The origin of palsas, Geografiska Annaler. Series A. Physical Geography, 1986.

Soliman, A., Duguay, C., Saunders, W., and Hachem, S.: Pan-Arctic Land Surface Temperature from MODIS and AATSR: Product Development and Intercomparison, Remote Sensing, 4, 3833–3856, doi:10.3390/rs4123833, 2012.

Takala, M., Luojus, K., Pulliainen, J., Derksen, C., Lemmetyinen, J., Kärnä, J.-P., Koskinen, J., and Bojkov, B.: Estimating northern hemisphere snow water equivalent for climate research through assimilation of space-borne radiometer data and ground-based measurements, Remote Sensing of Environment, 115, 3517 – 3529, doi:https://doi.org/10.1016/j.rse.2011.08.014, http://www.sciencedirect.com/science/article/pii/S0034425711003166, 2011.

Trofaier, A. M., Westermann, S., and Bartsch, A.: Progress in space-borne studies of permafrost for climate science: Towards a multi-ECV approach, Remote Sensing of Environment, doi:https://doi.org/10.1016/j.rse.2017.05.021, 2017.

Wang, L., Derksen, C., and Brown, R.: Detection of Pan-Arctic Terrerstrial Snowmelt from QuikSCAT, 2000-2005, Remote Sensing of Environment, 112, 3794–3805, 2008.
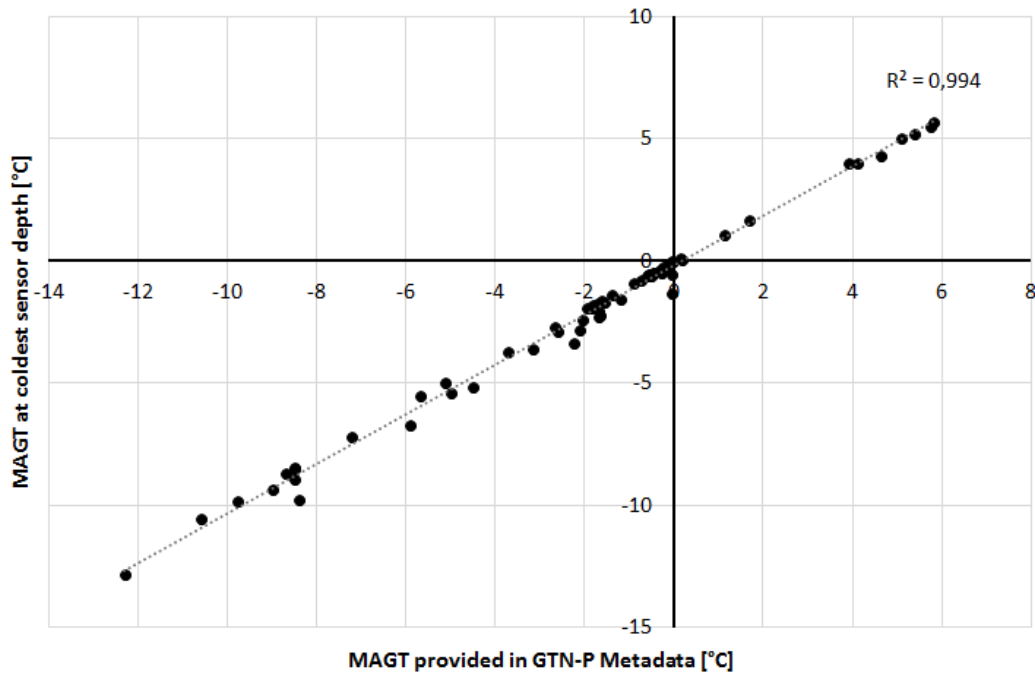
Figure 1. Mean Annual Ground Temperature (MAGT) derived from GTN-P metadata versus derived MAGT from coldest sensor (for year specified in the meta data). Dotted line represents linear fit.

Westermann, S., Østby, T., Gisnås, K., Schuler, T., and Etzelmüller, B.: A ground temperature map of the North Atlantic permafrost region based on remote sensing and reanalysis data, Cryosphere, 9, 1303–1319, doi:10.5194/tc-9-1303-2015, 2015.

Woo, M., Kane, D. L., Carey, S. K., and Yang, D.: Progress in permafrost hydrology in the new millennium, Permafrost and Periglacial Processes, 19, 237–254, doi:10.1002/ppp.613, 2008.

5 Zhang, T., Frauenfeld, O. W., Serreze, M. C., Etringer, A., Oelke, C., McCreight, J., Barry, R. G., Gilichinsky, D., Yang, D., Ye, H., Ling, F., and Chudinova, S.: Spatial and temporal variability in active layer thickness over the Russian Arctic drainage basin, Journal of Geophysical Research: Atmospheres, 110, n/a–n/a, doi:10.1029/2004JD005642, d16101, 2005.

Zhang, T., Barry, R., Knowles, K., Heginbottom, J., and Brown, J.: Statistics and characteristics of permafrost and ground-ice distribution in the Northern Hemisphere, Polar Geography, 31, 47–68, doi:10.1080/10889370802175895, 2008.

10 Zwieback, S., Paulik, C., and Wagner, W.: Frozen Soil Detection Based on Advanced Scatterometer Observations and Air Temperature Data as Part of Soil Moisture Retrieval, Remote Sens, 7, 3206–3231, doi:10.3390/rs70303206, 2015.
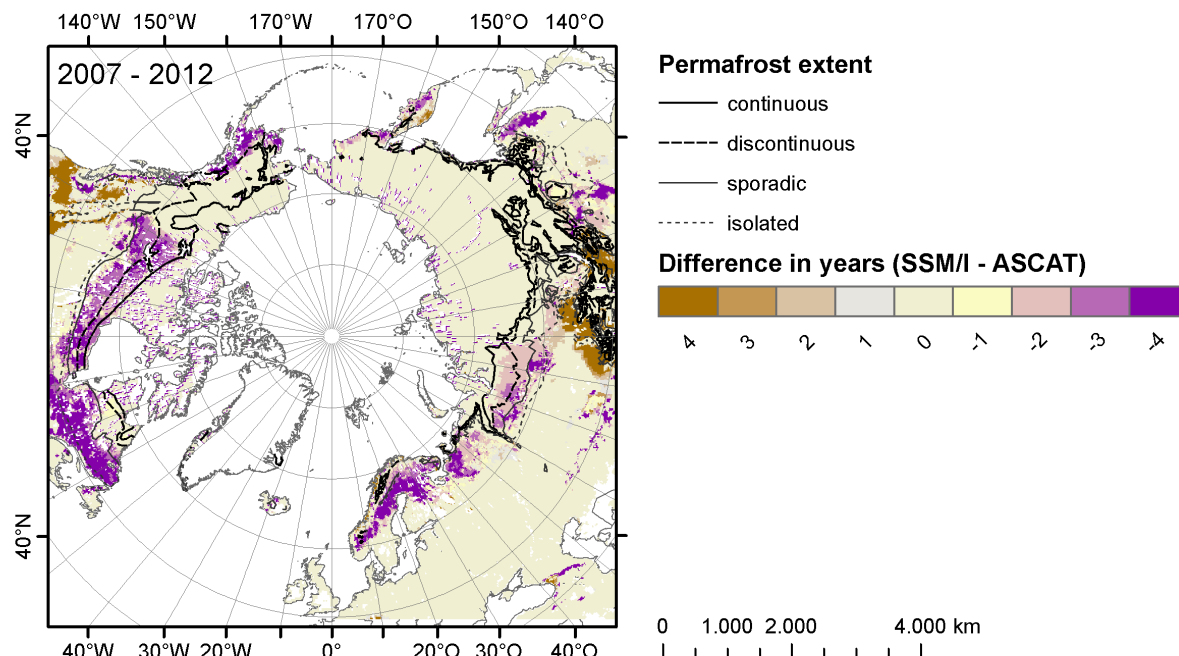
Figure 2. Comparison of the total number of years classified as permafrost between Metop ASCAT and SSM/I for 2008-2012 based on the 180 day threshold method applied to all years (minimum of two consecutive years with at least 180 days frozen).

Table 3. Permafrost extent comparison of satellite data results from Metop ASCAT based on modified thresholds (180, 190, 200 and 210 days) with permafrost extent classes from Brown et al. (1997). Covered area is provided in km^2 within each class. FT - days identified as frozen without melting snow are used, FM - days with melting snow are considered as frozen ground with Metop ASCAT. SSM/I classification results based on 180 days is included for comparison.

	IPA	FT 180	FT 190	FT 200	FT 210	FM 180	FM 190	FM 200	FM 210	SSMI 180
continuous [Mio. km²]	10.90	10.31	10.25	10.16	9.93	10.31	10.26	9.96	9.97	8.49
% of IPA		95%	94%	93%	91%	95%	94%	91%	92%	78%
discontnuous [Mio. km²]	2.97	2.71	2.13	1.49	0.86	2.73	2.20	1.57	1.03	2.11
% of IPA		25%	20%	14%	8%	25%	20%	14%	9%	19%
isolated [Mio. km²]	3.24	3.10	2.94	2.70	2.21	3.11	2.96	2.74	2.32	2.74
% of IPA		28%	27%	25%	20%	28%	27%	25%	21%	25%
sporadic [Mio. km²]	3.29	2.54	1.95	1.35	0.73	2.58	2.02	1.39	0.87	1.71
% of IPA		23%	18%	12%	7%	24%	19%	13%	8%	16%

Table 4. Comparison of satellite data results based on a 180 day threshold with permafrost extent from Brown et al. (2007). Covered area in % inside and outside permafrost regions is provided. FT - days identified as frozen without melting snow are used, FM - days with melting snow are considered as frozen ground with Metop ASCAT.

	ASCAT FT 180	ASCAT FM 180	SSMI FM 180
inside IPA	20.40	17.41	12.54
% of IPA	100%	85%	61%
outside IPA	0.00	-1.97	-1.09
% of IPA	0%	-10%	-5%
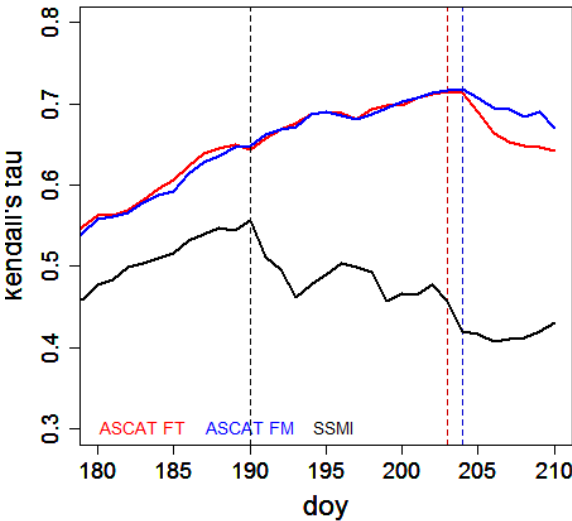
Figure 3. Curves of correlation coefficient (Kendall's τ) between 180 and 210 day of year (doy) frozen from satellite products and positive or negative MAGT at depth of coldest sensor from borehole data. FT - days identified as frozen without melting snow are used, FM - days with melting snow are considered as frozen ground with Metop ASCAT.

Table 5. Comparison of satellite data results based on based on modelled ground temperatures with permafrost extent from Brown et al. (1997). Covered area in % inside and outside permafrost regions. FT - days identified as frozen without melting snow are used, FM - days with melting snow are considered as frozen ground, LM - model results.

	FM LM 2007	FM LM 2008	FT LM 2007	FT LM 2008	SSMI LM 2007	SSMI LM 2008
inside IPA	19.15	18.10	16.44	18.10	14.50	14.55
% of IPA	94%	89%	81%	89%	71%	71%
outside IPA	5.90	4.78	2.98	4.78	3.08	2.40
% of IPA	-29%	-23%	-15%	-23%	-15%	-12%
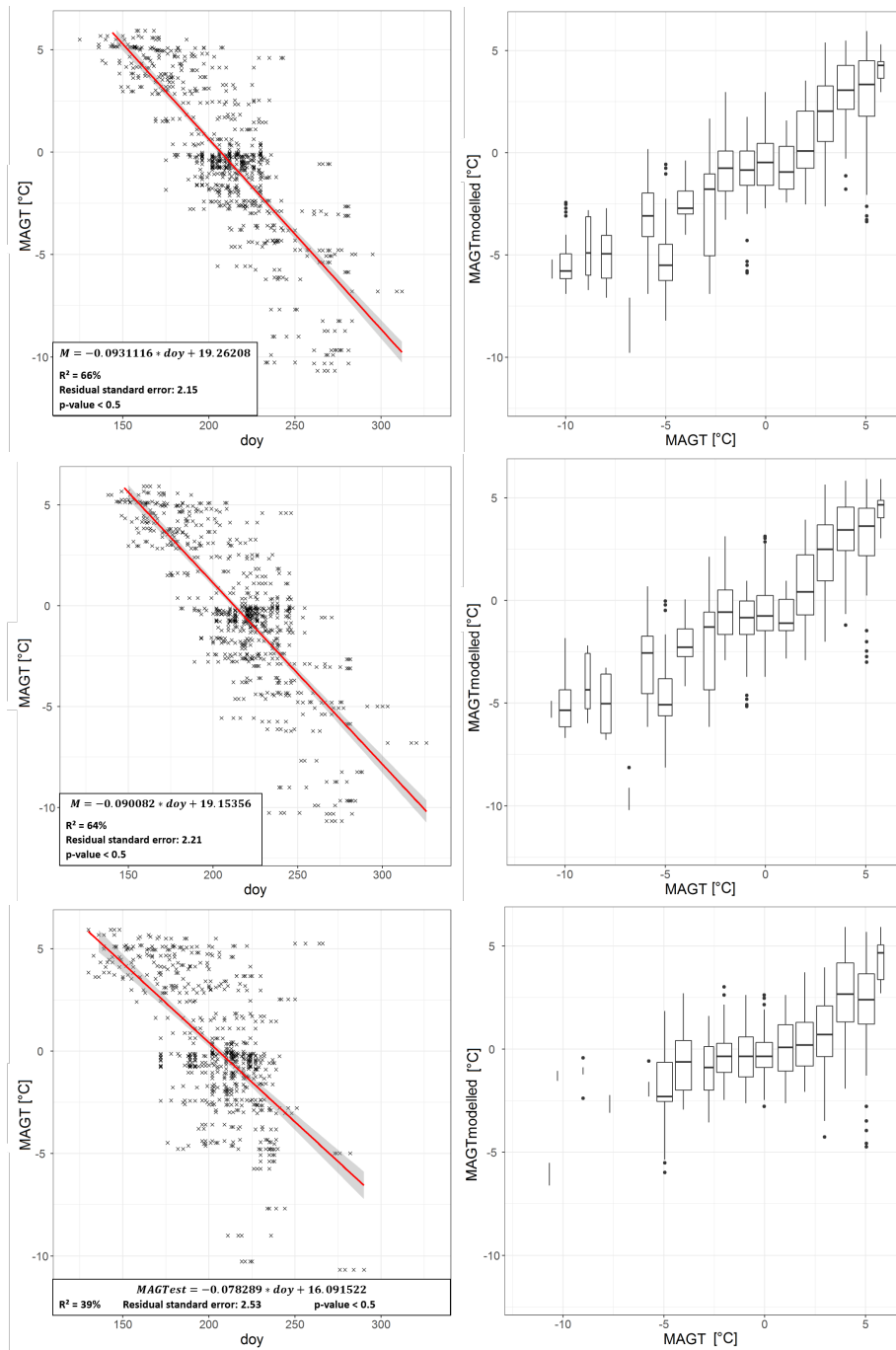
Figure 4. Left: Comparison of number of frozen days (doy - days of year) from satellite records and Mean Annual Ground Temperature for GTN-P boreholes (at depth of coldest sensor, years 2010-2012). Red line represents linear fit. Right: Box plots of modeled versus Mean Annual Ground Temperature from GTN-P boreholes (at depth of coldest sensor, years 2007/8 and 2008/9) Top: ASCAT excluding snow melt days, middle: ASCAT with snow melt days, bottom: SSM/I.
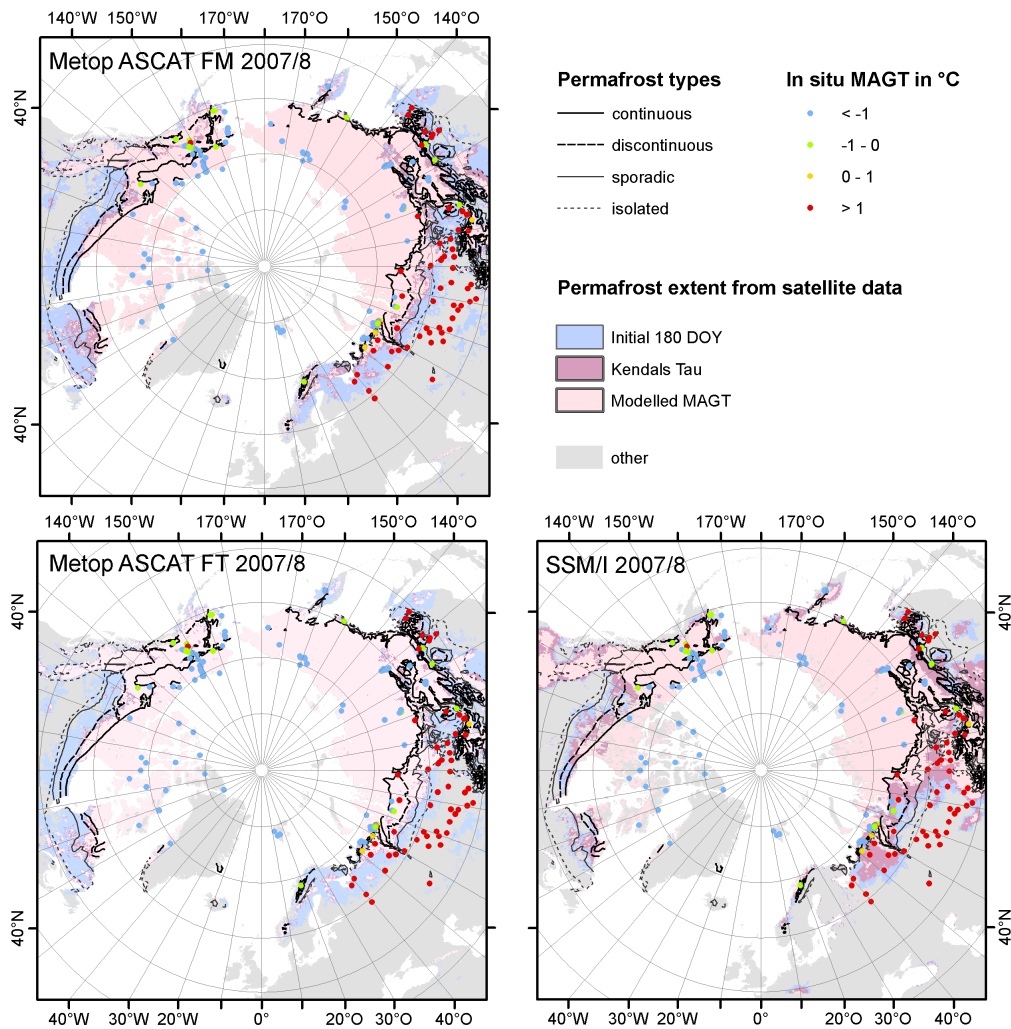
Figure 5. Permafrost extent maps based on thresholds applied to frozen days of year (DOY) to ASCAT excluding melt days (FT), thresholds applied to frozen days of year (DOY) to ASCAT including melt days (FM), and thresholds applied to frozen days of year (DOY) to SSM/I. The initial threshold is 180 days. The value for best Kendall's τ represents the best fit with borehole measurements. The highest threshold has been determined using an empirical model calibrated with borehole measurements. See also Table 2. All satellite results are based on 2007/8-2008/9 records. Source for permafrost extent classes: Brown et al. (1997).
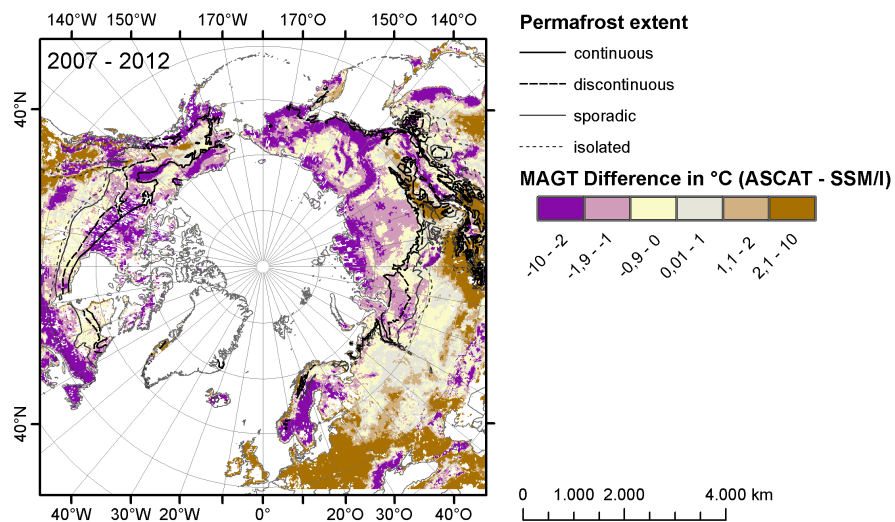
Figure 6. Comparison of MAGT in °C of all years between Metop ASCAT (FT) and SSM/I for 2007-2012. Source of permafrost extent classes: Brown et al. (2007).
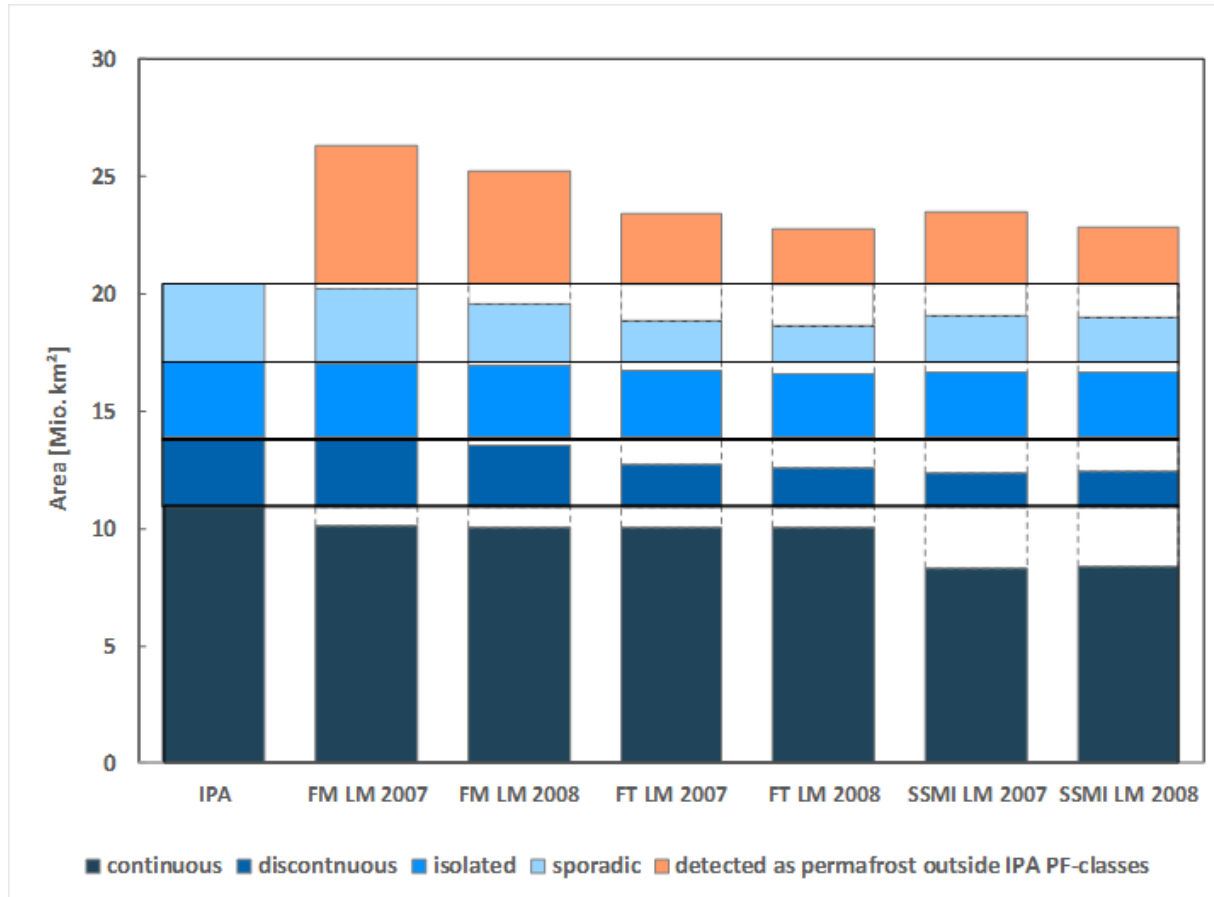
Figure 7. Permafrost extent comparison of satellite data results based on modelled ground temperatures (LM - Linear Model) with permafrost classes from Brown et al. (1997). Covered area in km^2 within each class and outside. FT - days identified as frozen with ASCAT, FM - days with melting snow are considered as frozen ground with ASCAT.
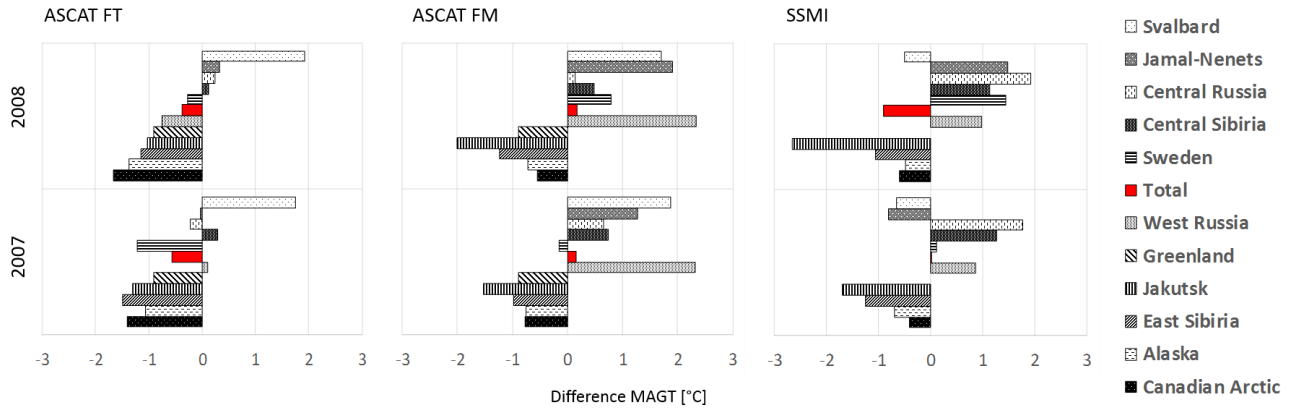
Figure 8. Difference between in situ MAGT (coldest sensor) and modelled MAGT by region (see Fig. A1) in 2007/8 and 2008/9. FT - days identified as frozen without melting snow are used, FM - days with melting snow are considered as frozen ground in ASCAT.
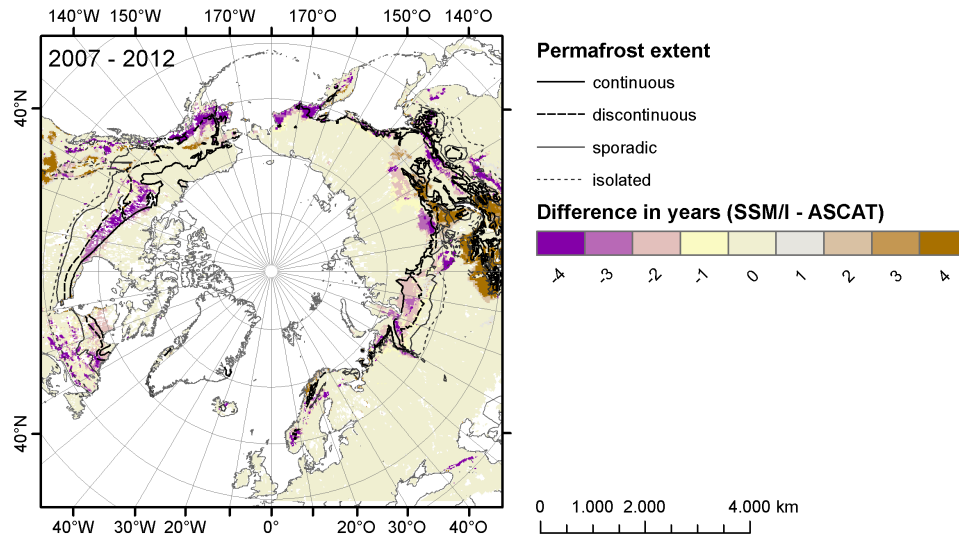
Figure 9. Comparison of the total number of years classified as permafrost between Metop ASCAT (FT) and SSM/I for 2008-2012 based on the zero degree temperature threshold method applied to all years (minimum of two consecutive years with below zero degree). Source of permafrost extent classes: Brown et al. (2007).
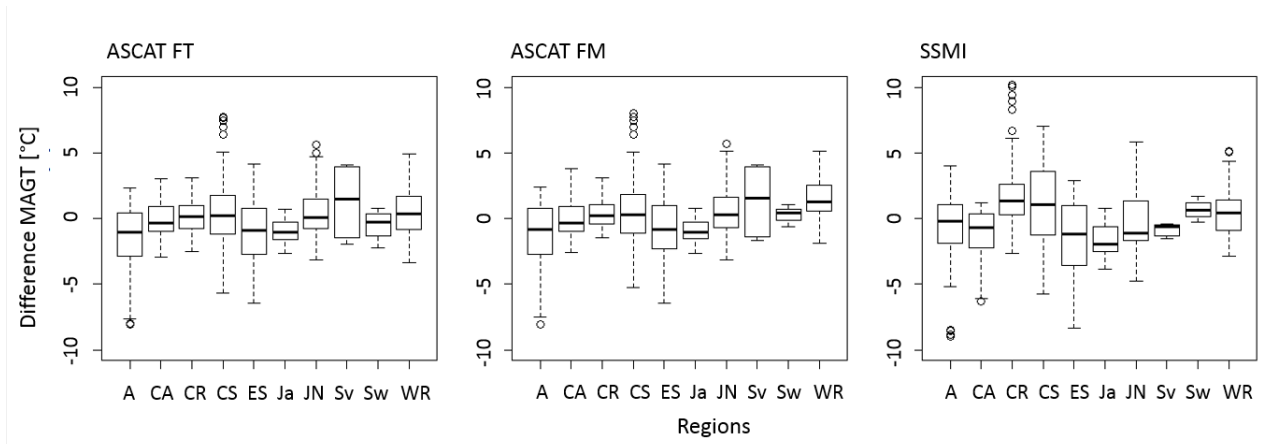
Figure 10. Difference between in situ MAGT (coldest sensor) and modelled MAGT by region (see Fig. A1) for all years. Only stations which overlap with records from all datasets are considered. FT - days identified as frozen without melting snow are used, FM - days with melting snow are considered as frozen ground in ASCAT.
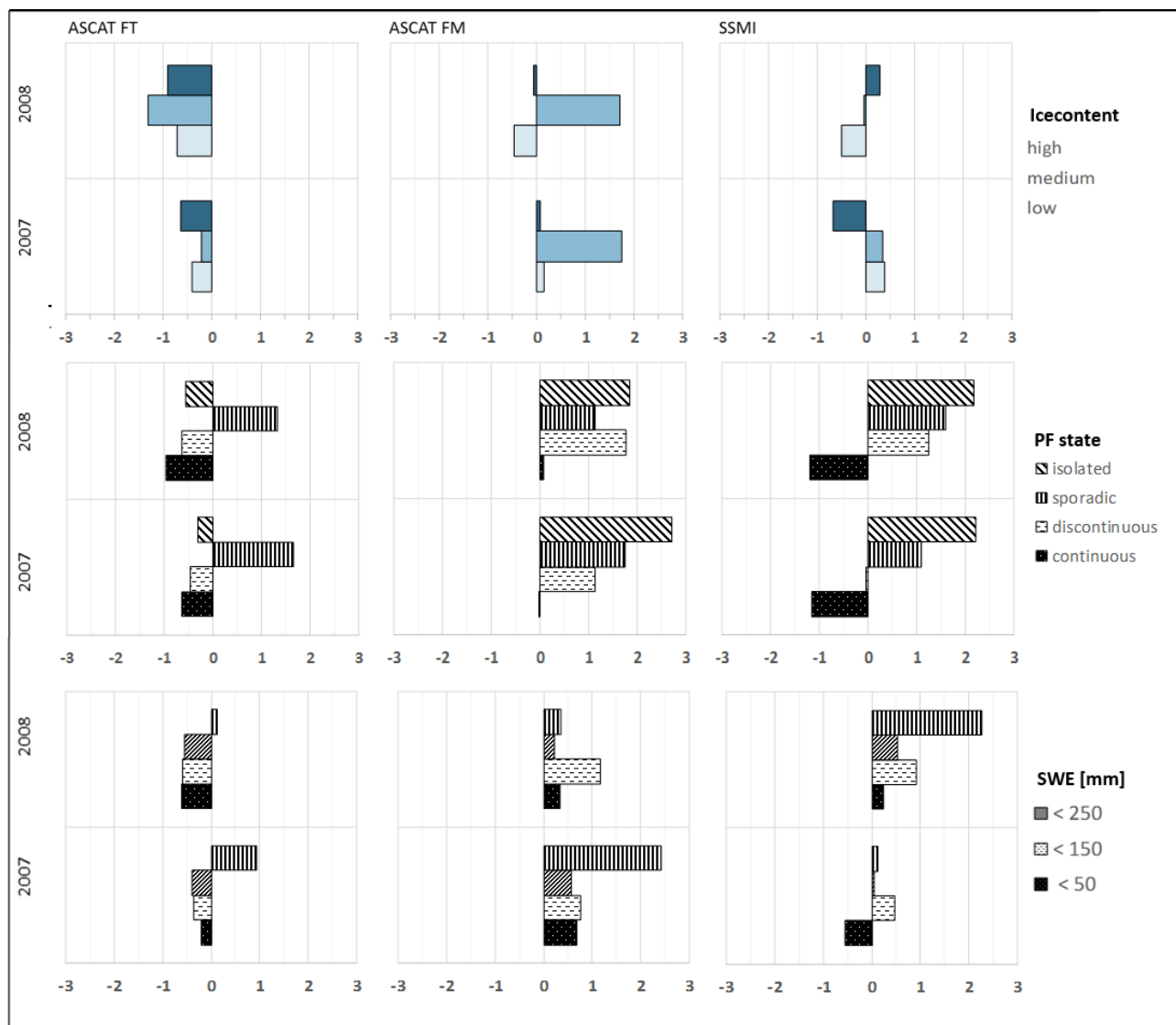
Figure 11. Difference between in situ MAGT (coldest sensor) and modelled MAGT by permafrost zone and ice content (source: Brown et al. (1997)), and snow water equivalent (SWE, source: GlobSnow) categories in 2007/8 and 2008/9. FT - days identified as frozen without melting snow are used, FM - days with melting snow are considered as frozen ground in ASCAT.
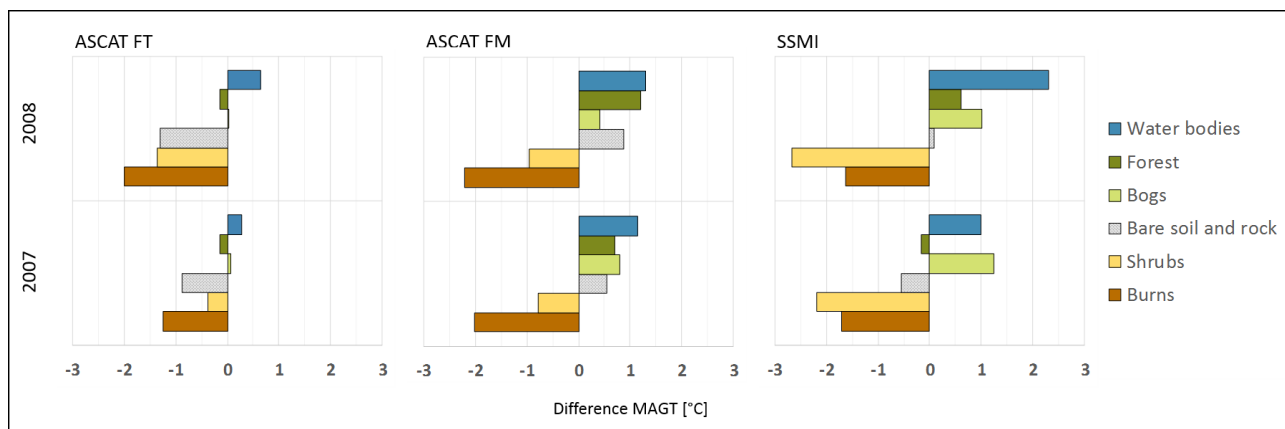
Figure 12. Difference between in situ MAGT (coldest sensor) and modelled MAGT by land cover type (source: GLC2000 (2003)) in 2007/8 and 2008/9. FT - days identified as frozen without melting snow are used, FM - days with melting snow are considered as frozen ground in ASCAT.
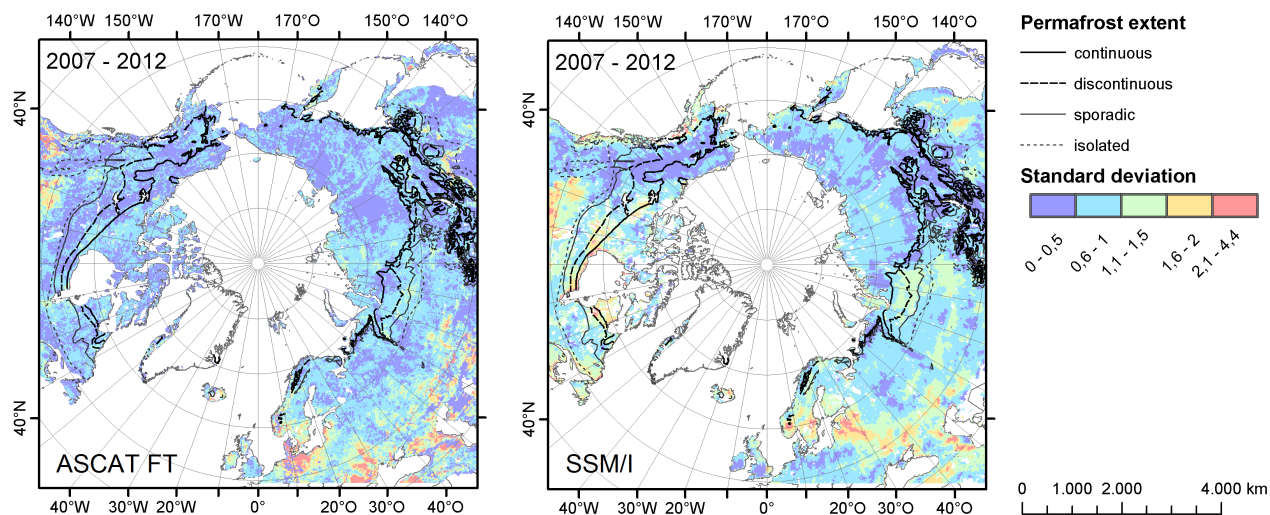
Figure 13. Maps of standard deviation of modelled MAGT for ASCAT excluding melt days (FT) and SSM/I based on all analyzed years. Source for permafrost extent classes: Brown et al. (1997).

Appendix A
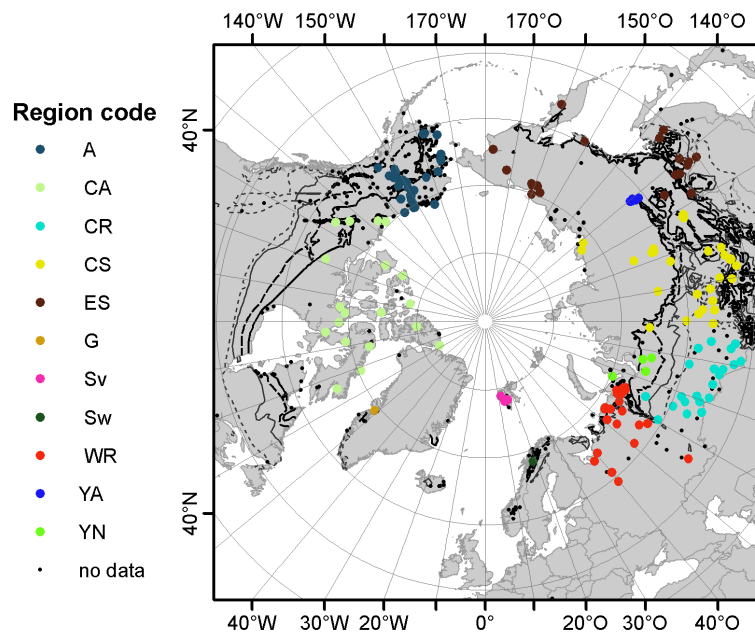
Figure A1. Map of used GTN-P boreholes with region class. 'No data' refers to sites without publicly available data or sites which failed the selection criteria. A - Alaska, CA - Canada, CR - Central Russia, CS - Central Siberia, ES - Eastern Siberia, G - Greenland, Sv - Svalbard, Sw - Sweden, WR - Western Russia, YA - Yakutia, YN - Nenets.
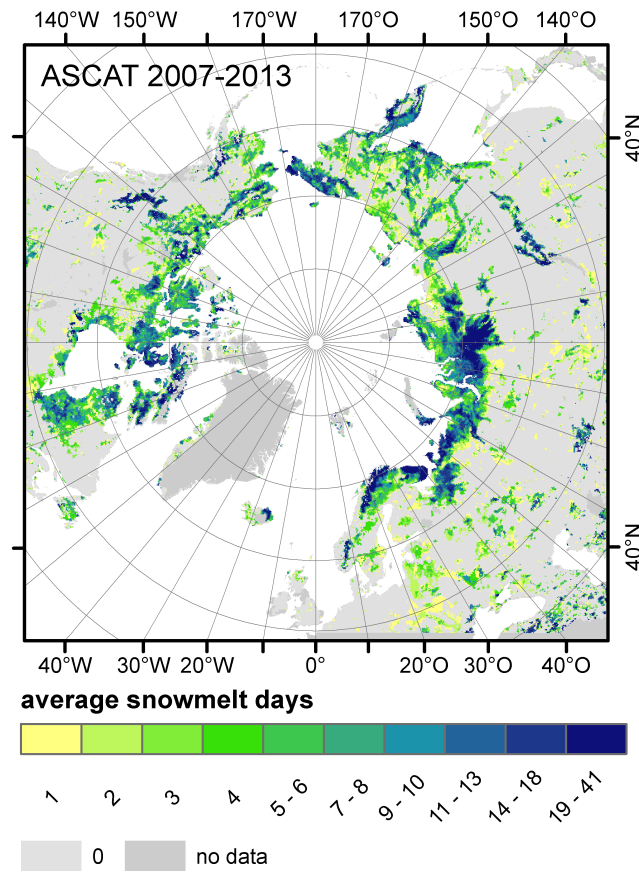
Figure A2. Average number of snow melting days per year from Metop ASCAT for 2007 – 2013 derived from Paulik et al. (2014).